

**Letter of Intent**  
**ELECTROMAGNETIC PROCESSES IN STRONG CRYSTALLINE FIELDS**

J.U. Andersen, S.P. Møller, A.H. Sørensen, E. Uggerhøj, U.I. Uggerhøj  
Department of Physics and Astronomy, Aarhus University, Denmark

A. Apyan  
Department of Physics and Astronomy, Northwestern University, Evanston IL, USA

S. Ballestrero, P. Sona  
Institute of Physics, Florence University, Italy

S. Connell  
Schonland Research Institute, Johannesburg, South Africa

T. Ketel  
Science Department, Free University, Amsterdam, The Netherlands

M. Khokonov  
Department of Physics, Kabardino-Balkarian State University, Nalchik, Russian Fed.

V. Biryukov, Yu. Chesnokov  
Institute of High Energy Physics, Protvino, Russia

W. Greiner, A.V. Korol, A.V. Solov'yov  
Frankfurt Institute for Advanced Studies, Johann Wolfgang Goethe University, Frankfurt, Germany

V. Baier  
Budker Institute of Nuclear Physics, Novosibirsk, Russia

S. Kartal, A. Dizdar  
Department of Physics, University of Istanbul, Turkey

A. Mangiarotti  
Physikalisches Institut, Heidelberg, Germany

**Abstract**

We propose a number of new investigations on aspects of radiation from high energy electron and positron beams (10-300 GeV) in single crystals. The common heading is radiation emission by electrons and positrons in strong electromagnetic fields, but as the setup is quite versatile, other related phenomena in radiation emission can be studied as well.

The intent is to clarify the role of a number of important aspects of radiation in strong fields as e.g. observed in crystals. We aim to measure trident 'Klein-like' production in strong crystalline fields, 'crystalline undulator' radiation, 'sandwich' target phenomena as well as axial and planar effects in contributions of spin to the radiation.

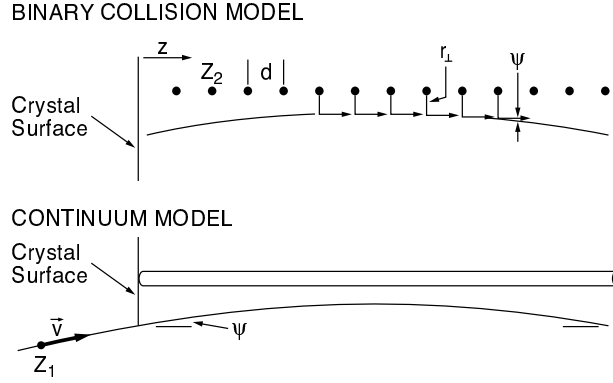


Figure 1: A schematic drawing of the discrete atomic scattering centers in a crystal and the continuum approximation. The target atoms with atomic number  $Z_2$  and distance  $d$  along the string, impose a curved trajectory on the penetrating particle with atomic number  $Z_1$  through binary encounters over the transverse distance  $r_{\perp}$ . The resulting trajectory with entrance angle  $\psi$  can be accurately described as the result of interaction with a string of continuous charge distribution, corresponding to a ‘smearing’ of the charges  $Z_2e$  along the direction  $z$  of the rows of atoms.

## 1 Introduction

In the 1990’s, the NA43 collaboration [1] investigated a number of phenomena in strong field QED among which can be mentioned: radiation emission in crystals [2], pair production [3], shower formation [4], axial radiative cooling [5] and the influence of spin on the radiation [6]. The knowledge gained on radiation processes by this collaboration has stimulated substantial activity in theoretical [7, 8] as well as in related experimental areas that now render it very desirable to extend the measurements and pursue new phenomena.

Under small angles of incidence to a crystallographic direction - an axis or a plane - the strong electric fields of the nuclear constituents add coherently such as to obtain a macroscopic, continuous field with a peak value of the order  $\mathcal{E} \simeq 10^{11}$  V/cm. Therefore, in the restframe of an ultrarelativistic electron with a Lorentz factor of  $\gamma \simeq 10^5$ , the field encountered becomes comparable to the critical (or Schwinger-) field,  $\mathcal{E}_0 = m^2c^3/e\hbar = 1.32 \cdot 10^{16}$  V/cm, corresponding to a magnetic field  $B_0 = 4.41 \cdot 10^9$  T. The incident particle moves in these immensely strong fields over distances up to that of the crystal thickness, i.e. up to several mm. Since the quantity

$$\chi = \gamma\mathcal{E}/\mathcal{E}_0 \quad (1)$$

is a relativistic invariant for the transverse field  $\mathcal{E}$ , the behaviour of charged particles in fields as strong as  $\mathcal{E}_0$  can be investigated by use of ultrarelativistic electrons in strong crystalline fields. Already at  $\chi \simeq 0.1$  the synchrotron-like radiation emission attains a non-classical character [6]. An introduction to these ‘strong field effects’ can be found in [9, 10].

In CERNs NA48 experiment two applications of strong crystalline fields have been used: An efficient conversion of photons into electron-positron pairs to delimit the fiducial region [11] and a bent crystal to deflect a well-defined fraction of the main beam to generate kaons [12]. The first of these effects relies on the field in the rest-frame of an emitting electron to be comparable to the magnitude of the Schwinger field. The second effect is due to deflection by the electric field from a plane of crystal atoms which is equivalent to a magnetic field of up to a few thousand Tesla in the bent crystal. Clearly, the fields attained are exceedingly high and offer new possibilities in fundamental physics as well as applications. The proposed measurements will significantly enhance the understanding of QED processes in crystals and amorphous matter under special conditions, while also yielding insight into processes of astrophysical and practical importance, e.g. beamstrahlung, creation of QCD jets or radiation from highly magnetized neutron stars.

## 2 Strong crystalline fields

Three dimensionless invariants  $\chi$ ,  $\Xi$ ,  $\Gamma$  can be constructed from the electromagnetic field strength tensor,  $F_{\mu\nu}$ , and the momentum four-vector  $p^\nu$  (or, in the case of a photon,  $\hbar k^\nu$ ). For an ultra-relativistic particle moving across fields  $\mathcal{E} \ll \mathcal{E}_0$ ,  $B \ll B_0$  with an angle  $\theta \gg 1/\gamma$  the invariants fulfill  $\chi \gg \Xi, \Gamma$  and  $\Xi, \Gamma \ll 1$ . The relation of  $\chi$  to the fields  $\vec{\mathcal{E}}$  and  $\vec{B}$  is given by [13]

$$\chi^2 = \frac{1}{\mathcal{E}_0^2 m^2 c^4} ((\vec{p} \times \vec{B} + E \cdot \vec{\mathcal{E}})^2 - (\vec{p}c \cdot \vec{\mathcal{E}})^2) \quad (2)$$

For an ultrarelativistic particle moving perpendicularly to a purely electric or purely magnetic field this reduces to

$$\chi = \frac{\gamma \mathcal{E}}{\mathcal{E}_0} \quad \text{or} \quad \chi = \frac{\gamma B}{B_0} \quad (3)$$

which is identical to eq. (1).

For the emission of radiation it is the trajectory that is decisive. Therefore, it is insignificant if the field responsible for the path is electric or magnetic and electric fields present in crystals may be used to investigate e.g. synchrotron radiation.

Since  $\chi$  is invariant,  $\gamma B$  (or  $\gamma \mathcal{E}$ ) is the same in any reference system and thus it is reasonable to transform to the electron frame. In this reference system by definition the Lorentz factor of the electron is 1 and the field present in the frame of the laboratory is boosted by  $\gamma = E/mc^2$ , where  $E$  is the energy of the electron in the laboratory. This means that the field in the rest-frame of the electron can become critical for achievable  $\gamma$ -values.

## 3 Proposed measurements

In the following we discuss each of the sub-experiments in view of their relevance and recent activities, theoretical as well as experimental.

### 3.1 Klein-like trident production

Oscar Klein was one of the first to do calculations using the Dirac equation. In 1929 he looked at the probability of reflection of an electron from a steep potential barrier supplied by an electric field. He and others found that the probability for reflection exceeded 1 for electric fields beyond  $m^2 c^3 / e \hbar$ , i.e. when the field is so high that an electron transported over a Compton wavelength yields  $mc^2$ . Nowadays, this process is understood as pair production, which - without knowledge of the positron - was an impossible conclusion for Klein and it is therefore known as the Klein paradox. Klein-like pair production is for example addressed in heavy ion collisions where the local field during the collision may become ‘supercritical’ resulting in pair production [14].

Lately, the interest in the Klein paradox has been revived through theoretical studies with wave-packets [15] and space-time resolved simulations [16] that reach very different conclusions concerning the probability of positron production by electrons,  $e^- \rightarrow e^- e^+ e^-$  so-called trident production, in a strong field. In [16] it is claimed that ‘the incoming electron suppresses the pair production’.

Due to the invariance of the parameter  $\chi = \gamma \mathcal{E} / \mathcal{E}_0$ , it is possible to probe field strengths of the order of those relevant for the Klein paradox in single crystals. The only difference in the three dimensionless invariants describing the problems of trident production in crystals and the Klein paradox is that in the latter case  $\Xi$  - expressing the ‘inherent’ field strength - is of the order one. The relation  $\chi \gg \Xi, \Gamma$  still holds for both cases.

In fact, calculations of the drastic increase of trident production in crystals compared to an amorphous material has been existing for almost two decades [17]. One result is shown in fig. 2. A measurement of the trident production process requires the use of several thicknesses of foils, since the competing process where the electron radiates a *real* photon that subsequently produces a pair depends on the square of the thickness whereas trident production has a linear dependence. Furthermore, the ratio of probabilities for trident production to that of the cascade process involving a real photon in the intermediate step can be estimated as the ratio of the formation length to the target thickness,  $l_f / \Delta t_f$  [7] such that the required foil thickness must be of the order one formation length. This is a rather modest thickness - even for a 250 GeV electron producing a 1 GeV pair it is 0.1 mm, but it is still possible to discern the signal

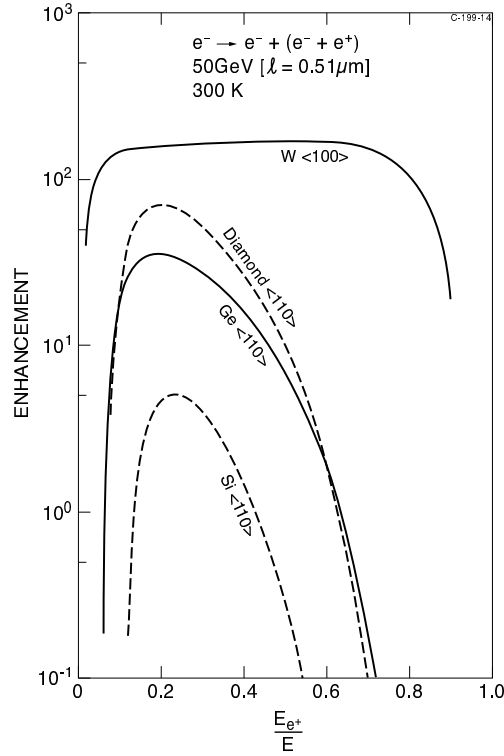


Figure 2: Enhancement of aligned over random incidence for trident production of four different crystals. The electron energy is 50 GeV and the horizontal scale is the fractional energy taken by the positron. Adapted from [17].

from background effects, in particular because of the huge enhancement and the fact that it increases with increasing energy of the primary electron. A full measurement is expected to be possible with about one week of beam time.

### 3.2 Crystalline Undulator

With a super-periodicity imposed by either ultra-sound [18], strain in Si-Ge interfaces [20] or surface defects [21] it is theoretically possible to generate high-intensity, nearly mono-chromatic radiation in a crystalline undulator [22, 23], see figure 3. A detection of the generated undulator-like radiation will constitute a proof-of-principle of this novel type of ‘insertion device’. Again, it is the very strong crystalline fields that boost the photon frequencies to much higher values, see figure 4, while at the same time requiring much less space, of the order few mm.

Although it is advantageous to use positrons to generate radiation (because of decreased multiple scattering under channeling conditions) [23], we wish as well to investigate the behaviour of electrons. With a week of beam time for this sub-experiment, we would be able to run with two different crystals, testing the different approaches to produce a crystalline undulator, with both positrons and electrons, and for several energies. We are presently studying methods to develop Si-Ge crystals by means of Molecular Beam Epitaxy.

### 3.3 Axial and planar investigations of spin-flip radiation

The effect of spin on the radiation for near-critical magnitudes of the field in the rest-frame of the emitting electron has been tested only in the axial case and for a relatively thick crystal. This may be extended to investigate planar effects as well as axial for thin crystals. The planar case for positrons is much more well-defined since the number of initially channeled particles is high, about 90% as opposed to barely 5% for axially channeled electrons.

Asymptotically, the spin contribution becomes  $\xi dN/d\xi \propto (\xi^7/(1-\xi))^{1/3} \cdot \chi^{2/3}$  for  $\chi \rightarrow \infty$  such

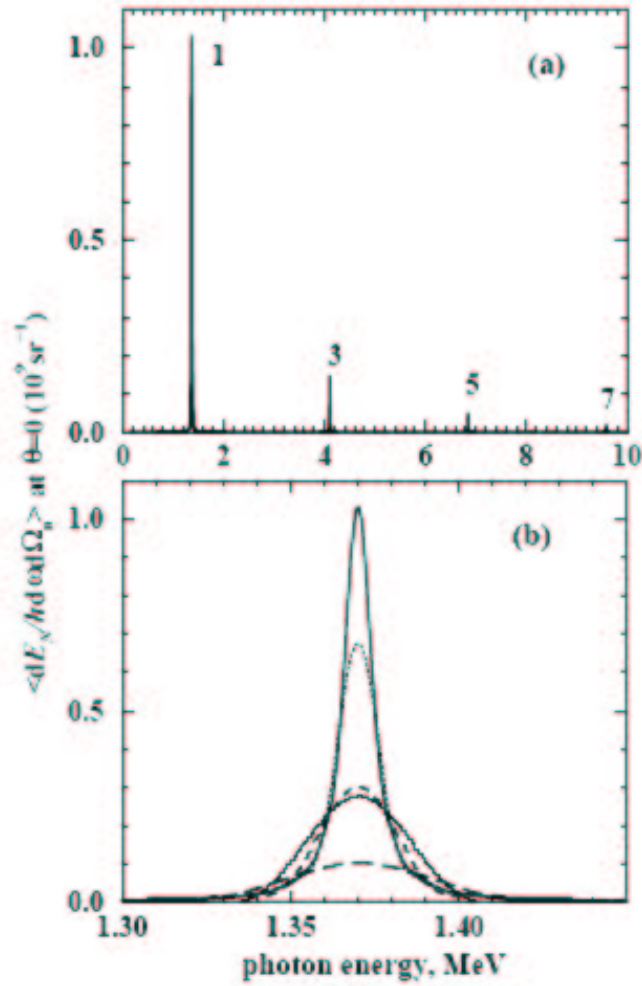


Figure 3: Spectral distribution of crystalline undulator radiation in the forward direction for 5 GeV positrons channeled in a 3.2 mm thick Si (110) crystalline undulator with  $N_d = 51$  periods. In (b) is shown the profiles of the first harmonics for  $N = 4N_d$  (solid),  $N = 2N_d$  (dots),  $N = N_d$  (dash),  $N = N_d/2$  (long-dash). Adapted from [19].

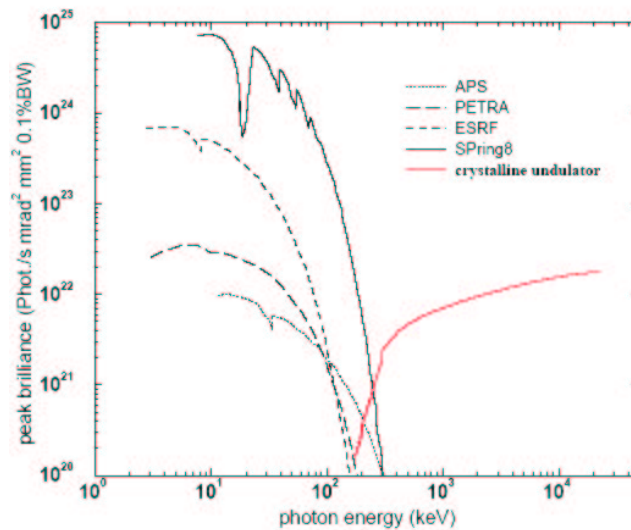


Figure 4: Peak brilliance of crystalline undulator radiation in the forward direction (red line) compared to conventional third generation light sources as indicated. From [24].

that it is strongly peaked at the upper end of the spectrum. An example is given in fig. 5 where the value of  $\chi$  is set to 100.

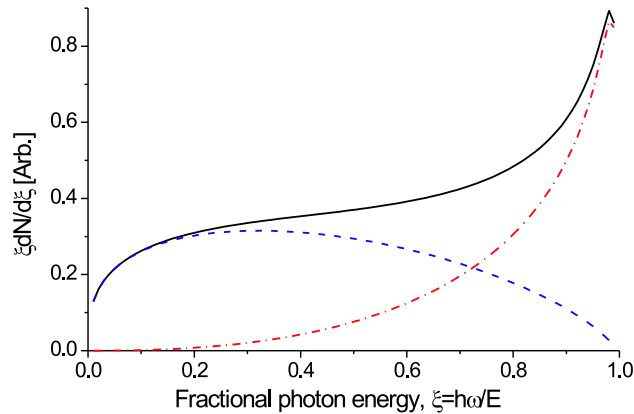


Figure 5: *Synchrotron radiation in a strong field, where the full line is the total spectrum, the dash-dotted line shows the contribution from the spin and the dashed line is obtained by neglecting the spin. The value of  $\chi$  is set to 100.*

The study of radiation emission for high values of  $\chi$  is relevant for e.g. beamstrahlung. The emission of beamstrahlung can be expressed as a function of  $\chi$  (often called  $\Upsilon$  in the accelerator physics community) which for the Stanford Linear Collider (SLC) is small  $\simeq 10^{-3}$  but of the order unity for the next generation linear colliders [25, 26]. The influence of spin on the radiation process [6, 27] becomes the dominant factor once  $\Upsilon$  or  $\chi$  becomes much higher than 1. We wish to do a measurement in two ‘cleaner’ cases, namely where the crystal is thin enough to make pile-up insignificant and in the case of planar channeled positrons, where the transverse potential is well approximated by a harmonic potential.

For a future linear collider operating in the ‘quantum regime’, the beamstrahlung spectrum becomes similar to the spectrum shown in fig. 5, see the full-drawn line in fig. 6.

### 3.4 Sandwich (structured) targets

Following the successful experimental test in H2 of the Landau-Pomeranchuk-Migdal (LPM) effect at high energies [29, 30], we wish to study the formation process of high energy photons. The basis of the LPM effect is the ‘formation length’ - the distance traversed by an electron during the emission of the photon. The formation length can be up to 100 microns, depending on electron and photon energy. Low energy photons have longer formation lengths. In the light of this we wish to ‘force’ the electron to emit high energy photons by passing it through a foil which is simply too thin for the emission of many low energy photons, i.e. the formation length is longer than the foil thickness [31]. This can be done by a ‘sandwich foil’ where about 50 foils of a few micron thick gold are interspersed by Low Density PolyEthylene (LDPE) which has a large radiation length and thus resembles air. By this technique we can achieve a target which is thick enough to yield a high signal-to-background in H4, yet each sub-target is thin enough to suppress photons below a limit of several GeV. The study is relevant in several contexts, e.g. heavy ion physics, linear collider technology, coherent bremsstrahlung and transition radiation. For the emission of soft gluons by a penetrating quark, the finite size of the nucleon may suppress the emission [32]. Second, taken to the extreme of energies as high as 4 TeV, a realistic sandwich target consisting of 7 micron thick sub-targets will suppress by a factor 2 the radiation below 2 TeV yielding a potential source of photons of very high energy with a reduced disturbance from low energy photons. Third, interferences from radiation amplitudes from subsequent foils in the stack can be studied in a scheme reminiscent of coherent bremsstrahlung, only with much larger interaction spacing [33]. Last, transition radiation dominated by multiple scattering can be studied. In this regime, a 200 GeV electron may emit transition radiation in the few-GeV region, way above the ‘classical’ transition radiation characterized

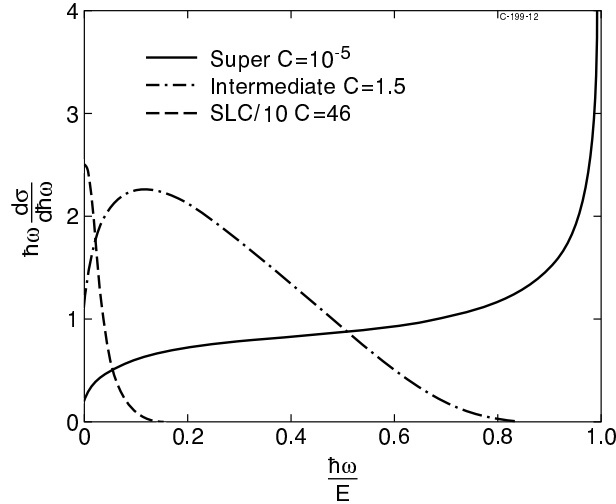


Figure 6: Three examples of beamstrahlung power spectra where the horizontal scale is the fractional photon energy and the constant  $C$  here is approximately equal to  $1/\chi$ . Adapted from [28].

by  $\gamma\hbar\omega_p$ , about 3 MeV in e.g. Au with plasma frequency  $\omega_p = 80 \text{ eV}/\hbar$ . Preliminary studies performed during the ‘Chudakov’ test in H4, 2004 show that these measurements can be performed with relatively little beam time, about one week.

#### 4 Equipment and beam time

The equipment is existing, the beam is as used in NA43, i.e. 10-300 GeV electrons derived from  $50 \cdot 10^{12}$  POT, and we request from CERN to give access to the beam in H4 with 1 MBPL and 1 MDX magnets installed in the zone 134. To fully benefit from the similarity of the setup with that of NA43 and the desire to go to high energy (nominally 300 GeV) it is necessary to use the H4 beam. The possibility of going to high energies (above 200 GeV) with an essentially parallel beam is essential to some of the proposed measurements. Therefore, CERN is the only place these experiments can be performed.

The presented scheme relies solely on QED processes. The comparatively high cross sections for these processes - even for higher order contributions - mean that datataking time in each case is rather limited, of the order a few days, depending on the target.

We estimate the setup and calibration time to be 5 days, so all of the measurements can be performed within a total period of  $2 \times 3$  weeks, e.g. in 2006 and 2007, with a setup closely analogous to that of NA43 (see below).

#### 5 Experiment

The proposed experimental setup is shown in figure 7. Its main components are 6 drift chambers, (DCs). DC1, DC2 and DC3 defines the entry- and exit-angles and positions on the first target, either crystalline or amorphous. DC4, downstream of the MBPL (shown as B8) is used as a tagging system where the primary  $e^+/e^-$  are deflected, and the radiated energy is found. This is also determined from a downstream lead glass array. Finally, DC5 and DC6 are placed downstream of an MDX (shown as Tr6) in front of which a conversion crystal or foil is positioned.

The last two drift chambers and the magnet are used as a magnetic pair spectrometer to determine the momentum of the pair produced in the converter - and thus the momentum of the photon. Moreover, by use of the lepton tracks in DC5 and DC6, the photon conversion vertex can be found with high accuracy, giving the possibility of measuring photon scattering angles. In NA43 [2] photon emission angles were determined.

In front of the second target, a scintillator (shown as Sc9), is positioned to reject those events where a photon has converted upstream. Immediately downstream of the second target, two counters, a solid-state detector (SSD) and a scintillator, Sc11, detect the pairs produced in the crystal. For normalization

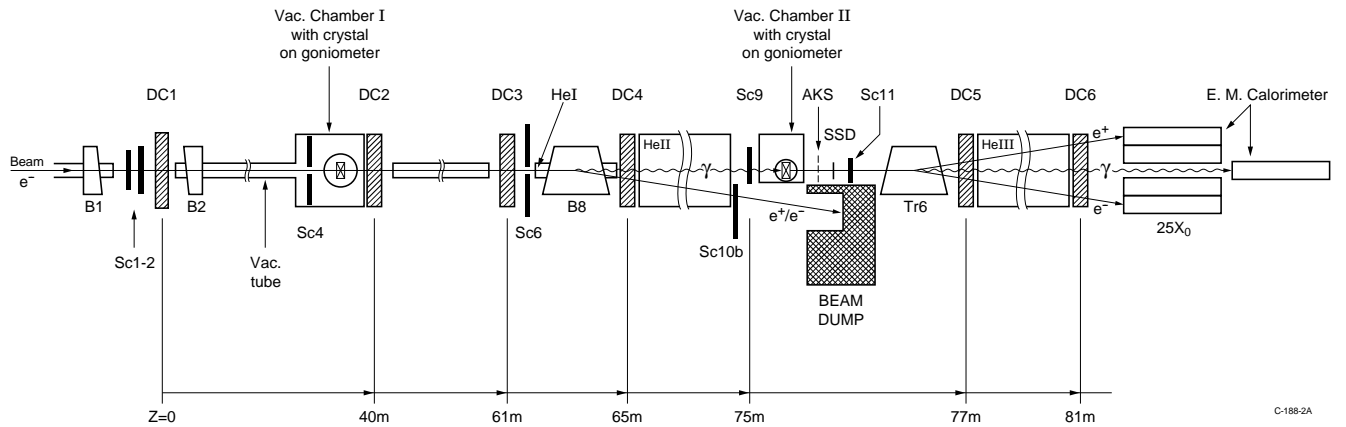


Figure 7: A schematic drawing of the setup used in NA43. See text for details.

and background subtraction random (non-aligned) directions and ‘no target’ measurements are to be performed. The leadglass detector array has a resolution of 7% (FWHM) at 149 GeV.

In the pair spectrometer used for photon multiplicities the minimum photon energy should be around 0.5 GeV, determined by the field in the MDX magnet. In the case of trident production this allows pairs with the desired formation length to be studied, while perturbing the trajectory of the primary electron very little.

## 6 Outlook

As shown above we will be able to address several important questions in the physics of radiation processes at high energies with a given beam time of only  $2 \times 3$  weeks. Once the setup is completed, it is essentially just a matter of changing the targets to investigate new phenomena. The investigations have implications in a broad range of contexts, ranging from basic QED processes in strong fields and quantum aspects of beam physics through investigations of air-showers to potential beam diagnostics devices, as discussed above. The proposed measurements will supplement and strengthen the conclusions reached by NA43 and since the setup is very similar to that of NA43 we benefit from having run most of the equipment several times before.

## References

- [1] E. Uggerhøj (spokesman, NA43), CERN/SPSC 90-31-SPSC/P234; K. Kirsebom *et al.*, CERN-SPSLC-96-5; SPSLC-M-572 (1996)
- [2] K. Kirsebom *et al.*, Nucl. Instrum. Methods B **174**, 274 (2001)
- [3] K. Kirsebom *et al.*, Nucl. Instrum. Methods B **135**, 143 (1998)
- [4] A. Baurichter *et al.*, Nucl. Phys. B (Proc. Suppl.) **44**, 79 (1995)
- [5] A. Baurichter *et al.*, Phys. Rev. Lett. **79**, 3415 (2001)
- [6] K. Kirsebom *et al.*, Phys. Rev. Lett. **87**, 054801 (2001)
- [7] V.N. Baier, V.M. Katkov and V.M. Strakhovenko, *Electromagnetic Processes at High Energies in Oriented Single Crystals*, World Scientific 1998.
- [8] M.Kh. Khokonov and H. Nitta., Phys. Rev. Lett. **89**, 094801 (2002)
- [9] A.H. Sørensen, Proc. NATO ASI **255**, 91, Plenum, 1991, reprinted in Nucl. Instr. Meth. B **119**, 1 (1996)
- [10] U.I. Uggerhøj, Rev. Mod. Phys., acc. for publ. (2005)
- [11] R. Moore *et al.*, Nucl. Instrum. Methods B **119**, 149 (1996)
- [12] N. Doble, L. Gagnon and P. Grafström, Nucl. Instrum. Methods B **119**, 181 (1996)
- [13] V.B. Berestetskii, E.M. Lifshitz and L.P. Pitaevskii, *Relativistic Quantum Theory*, Pergamon Press, New York, 1971.
- [14] W. Greiner, B. Müller and J. Rafelski - *Quantum Electrodynamics of Strong Fields*, Springer, Berlin 1985



- [15] H. Nitta, T. Kudo and H. Minowa, *Am. J. Phys.* **67**, 966 (1999)
- [16] P. Krekora, Q. Su and R. Grobe, *Phys. Rev. Lett.* **92**, 040406 (2004)
- [17] J.C. Kimball and N. Cue, *Phys. Rep.* **125**, 69 (1985)
- [18] A.V. Korol, A.V. Solov'yov and W. Greiner, *J. Phys.G: Nucl. Part. Phys.* **24**, L45 (1998)
- [19] A.V. Korol, A.V. Solov'yov and W. Greiner, *Int. J. Mod. Phys. E* **13**, 867 (2004)
- [20] U. Mikkelsen and E. Uggerhøj, *Nucl. Instr. Meth B* **160**, 435 (2000); R.O. Avakian *et al.*, in *Electron-Photon Interaction in Dense Media*, ed. H. Wiedemann (Kluwer, 2002)
- [21] S. Bellucci *et al.*, *Phys. Rev. Lett.* **90**, 034801 (2003)
- [22] R.O. Avakian *et al.*, *Nucl. Instr. Meth B* **173**, 112 (2001)
- [23] A.V. Korol, A.V. Solov'yov and W. Greiner, *Int. Journ. Mod. Phys. E* **8**, 49 (1999); W. Krause, A.V. Korol, A.V. Solov'yov and W. Greiner, *J. Phys.G: Nucl. Part. Phys.* **26**, L87 (2000); A.V. Korol, A.V. Solov'yov and W. Greiner, *J. Phys.G: Nucl. Part. Phys.* **27**, 95 (2001)
- [24] A.V. Korol, A.V. Solov'yov and W. Greiner, *Proc. Int. Workshop "Channeling 2004"*, physics/0412101 (2004)
- [25] A.V. Solov'yov, A. Schäfer and C. Hofmann, *Phys. Rev. E* **47**, 2860 (1993)
- [26] A.V. Solov'yov and A. Schäfer, *Phys. Rev. E* **48**, 1404 (1993)
- [27] A. Kh. Khokonov *et al.*, *Technical Physics* **47**, 1413 (2002); A. Korol, A.V. Solov'yov and W. Greiner, *J. Phys.G: Nucl. Part. Phys.* **28**, 627 (2002)
- [28] R. Blankenbecler and S.D. Drell, *Phys. Rev. D* **36**, 277 (1987)
- [29] H.D. Hansen *et al.*, *Phys. Rev. Lett.* **91**, 014801 (2003)
- [30] H.D. Hansen *et al.*, *Phys. Rev. D* **69**, 032001 (2004)
- [31] N.F. Shul'ga and S.P. Fomin, *JETP* **86**, 32 (1998); N.F. Shul'ga and S.P. Fomin, *JETP Lett.* **63**, 873 (1996)
- [32] B.Z. Kopeliovich, A. Schäfer and A.V. Tarasov, *Phys. Rev. C* **59**, 1609 (1999)
- [33] R. Blankenbecler, *Phys. Rev. D* **55**, 190 (1997); R. Blankenbecler and S.D. Drell, *Phys. Rev. D* **53**, 6265 (1996)